

# Degradation of target coverage due to inter-fraction motion during intensity-modulated proton therapy of prostate and elective targets

Sara Thörnqvist, Ludvig P. Muren, Lise Bentzen, Liv B. Hysing, Morten Høyer, Cai Grau & Jørgen B. B. Petersen

**To cite this article:** Sara Thörnqvist, Ludvig P. Muren, Lise Bentzen, Liv B. Hysing, Morten Høyer, Cai Grau & Jørgen B. B. Petersen (2013) Degradation of target coverage due to inter-fraction motion during intensity-modulated proton therapy of prostate and elective targets, Acta Oncologica, 52:3, 521-527, DOI: [10.3109/0284186X.2012.752860](https://doi.org/10.3109/0284186X.2012.752860)

**To link to this article:** <https://doi.org/10.3109/0284186X.2012.752860>



Published online: 14 Feb 2013.



Submit your article to this journal [↗](#)



Article views: 1441



View related articles [↗](#)



Citing articles: 8 View citing articles [↗](#)

## ORIGINAL ARTICLE

**Degradation of target coverage due to inter-fraction motion during intensity-modulated proton therapy of prostate and elective targets**SARA THÖRNQVIST<sup>1,2</sup>, LUDVIG P. MUREN<sup>1,2</sup>, LISE BENTZEN<sup>2</sup>, LIV B. HYSING<sup>3</sup>,  
MORTEN HØYER<sup>1,2</sup>, CAI GRAU<sup>1,2</sup> & JØRGEN B. B. PETERSEN<sup>1</sup><sup>1</sup>Department of Medical Physics, Aarhus University Hospital, Aarhus, Denmark, <sup>2</sup>Department of Oncology, Aarhus University Hospital, Aarhus, Denmark and <sup>3</sup>Department of Oncology and Medical Physics, Haukeland University Hospital, Bergen, Norway**Abstract**

Internal target and organ motion during treatment is a challenge in radiotherapy (RT) of the prostate and the involved elective targets, with residual motion being present also following image-guidance strategies. The aim of this study was to investigate organ motion-induced dose degradations for the prostate, seminal vesicle and the pelvic lymph node when treating these targets with proton therapy, using different image-guidance and delivery strategies. *Material and methods.* Four patients were selected from a larger series as they displayed large inter-fractional variation in bladder and rectum volume. Intensity-modulated proton therapy plans were generated using both simultaneous integrated and sequential boost delivery. For each technique, three isotropic margin expansions (in the range of 4–10 mm) were evaluated for the clinical target volume of prostate (CTV-p), seminal vesicles (CTV-sv) and lymph nodes (CTV-ln). Simulation of the dose degradations for all treatment plans were based on dose re-calculations for the 8–9 repeat CTs available for each patient, after applying rigid registrations to reproduce set-up based on either intra-prostatic fiducials or bony anatomy. *Results.* The simulated dose received by 99% of the target volume ( $D_{99}$ ) and generalized equivalent dose (gEUD) showed substantial inter-patient variations. For 40% of the investigated scenarios, the patient average simulated  $D_{99}$  for all targets were within 2 GyE from the planned dose. The largest difference between simulated and planned dose was seen for the CTV-sv when using SIB delivery, with an average relative reduction in  $D_{99}$  of 13% and 15% for the largest margin expansion, when positioned using fiducials and bony anatomy, respectively. *Conclusions.* The most severe dose degradations were found for CTV-sv, but they were also evident for CTV-ln. The degradations could not be completely resolved, neither by using the largest margin expansion nor with the choice of set-up. With fiducial set-up CTV-p was robust against the inter-fraction changes.

In radiotherapy (RT) of prostate cancer, improved treatment outcomes has been achieved through dose escalation enabled by implementation of increasingly more conformal delivery techniques [1–3]. Along this development, proton therapy is being used in the treatment of localized prostate cancer [4–8]. A large proportion of prostate cancer patients, those with locally advanced, high-risk disease, receive RT also to the pelvic lymph nodes, although there still are controversies both regarding the actual clinical evidence and the potentially elevated risk of complications [9]. The increased conformity that can be achieved with protons as compared to photons makes protons potentially beneficial when irradiating large

complex-shaped targets [10,11]. In this perspective, proton therapy for locally advanced prostate cancer is therefore attractive [12].

Previous RT planning studies for prostate cancer comparing photons to protons have documented both reduced integral doses [10,13] and lower dose to the involved organs at risk, the bladder, rectum and bowel [10,14]. For locally advanced prostate cancer a plan comparison showed equivalent target coverage combined with the expected reduced risk of rectum toxicity [10]. However, independent target movement and changes in anatomy as compared to the situation used for planning can be a challenge [15] for proton RT. Strategies to limit such effects

for prostate irradiation are not easily applicable to the often co-irradiated seminal vesicles and pelvic lymph nodes [16,17]. Based on the experience from an intensity-modulated RT (IMRT) robustness study [17], we now turn our attention to the organ motion-induced dose degradations for the three targets – the prostate, seminal vesicles and pelvic lymph nodes – in intensity-modulated proton therapy (IMPT). The evaluations were made for a selected group of the patients with large organ motion for the purpose of showing a worst case scenario of dosimetric consequences of inter-fraction organ motion, and were based on treatment simulations from dose re-calculation in a repeat CT-set. The investigations included both two image-guidance/positioning strategies – intra-prostatic fiducial markers versus bony anatomy – as well as two delivery techniques – sequential (SEQ) versus simultaneous integrated boost (SIB) – that are all in clinical use in photon RT of this patient group.

### Material and methods

Four patients were selected from a series of nine locally-advanced prostate cancer patients with repeat CT scans acquired during the course of RT [17,18]. The selection criteria was to include patients presenting the largest average relative reduction and relative increase when comparing rectum and bladder volumes of the repeat CTs to those in the planning CT (Figure 1). For the rectum we therefore selected one patient with an average relative reduction of 52% and one case with an average increase of 19%. For the bladder one selected case had an average relative reduction of 41% while

the other case had a relative increase of 94%, as compared the planning CT. The four selected patients had a planning CT and 8–9 repeat CT scans acquired in close connection with their treatment fractions, all with a slice thickness of 2–3 mm. All scans were acquired with the same CT scanner (Phillips Brilliant Big Bore) using the same Hounsfield Unit calibration curves, and with the patient in supine position using similar fixation as during treatment. All patients had three fiducial markers implanted in the prostate; for dose calculations, the electron density of these were set equivalent to PMMA (poly methyl methacrylate).

### Treatment planning

For the purpose of this study, one experienced radiation oncologist (LB) delineated the clinical target volumes of prostate (CTV-p), seminal vesicles (CTV-sv) and the pelvic lymph nodes (CTV-ln) in all CT scans for all patients (i.e. 38 scans in total). Further details of target and organ at risk delineations have been presented previously [17,18].

To assess the robustness towards and the magnitude of dose degradation for the selected patients, different isotropic margin expansions of either 4 mm, 7 mm or 10 mm were applied around each of the CTVs to form the respective planning target volumes (PTV). As CTV-sv and CTV-ln were prescribed to receive identical dose levels, they formed a joint PTV (PTV-ln/sv) when optimizing the treatment plans.

The Eclipse treatment planning system version 10.0.28 (Varian Medical Systems, Palo Alto, USA) were used for generating all IMPT plans (a total of 24 plans) and dose re-calculations (408 in total).

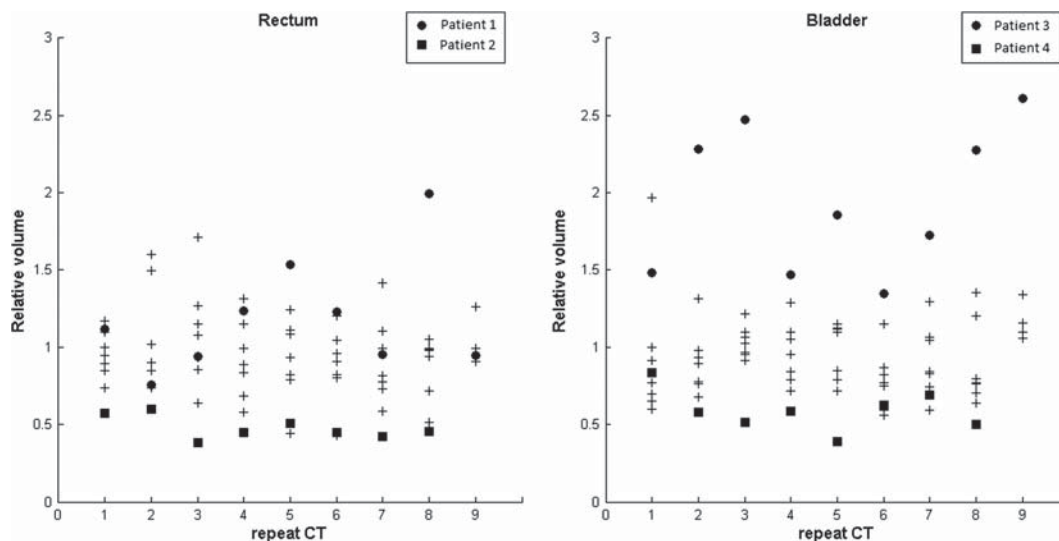


Figure 1. Relative change in volume compared to the planning CT across the repeat CT scans for the rectum and bladder. The data points of the four patients selected for this study are shown with solid symbols, the other with crosses.

The optimization was made using a simultaneous spot optimization algorithm similar to the algorithm developed by Lomax et al. [19]. The final dose calculation is based on a proton convolution superposition algorithm (Varian Medical Systems). For each patient, IMPT plans were created for the SEQ and SIB delivery, each with the different isotropic CTV-to-PTV expansions of 4 mm, 7 mm and 10 mm. Identical prescriptions to what was used for photon RT in our department was applied: 74 GyE to CTV-p and 55 GyE to CTV-In/sv, assuming a generic relative biological effectiveness of 1.1 for the proton prescriptions [20]. For the SIB plans, the two prescription levels were planned for delivery in 37 fractions, and for the SEQ plans 55 GyE was planned for delivery to all targets in 28 fractions with an additional 19 GyE/9 fraction-boost only to the prostate target. To evaluate the SEQ plans we used dose summation of the boost and the whole pelvic fields after dose re-calculation on each of the repeat CT scans. Hence, the SEQ plans used the same repeat CT scans twice, both for the boost fields and for the whole pelvic fields.

All IMPT plans used two lateral opposing fields ( $90^\circ$  and  $270^\circ$ ) and spot distributions calculated for a Cartesian grid encompassing the union of the two PTVs and extended with lateral margins of 5 mm. The spot-scanning technique was optimized for Gaussian spots with  $\sigma = 5$  mm and with both spot spacing and the spacing between scanning lines set to 5 mm. The highest priorities in the optimization were given to dose-volume objectives of: 1) the PTVs, to deliver homogenous target doses; and 2) the rectum, to reduce doses above 50 GyE, 70 GyE and 74GyE [17]. All treatment plans were normal-

ized to the mean dose of PTV-p and evaluated using the constraints published in a previous study [17]. An example of planned SEQ and SIB IMPT dose distributions are shown in Figure 2.

#### *Dose re-calculation and evaluation*

Simulation of proton delivery for the two positioning strategies was performed by transferring both the SEQ and SIB plans to each of the repeat CT scans utilizing the rigid registrations based on either the intra-prostatic gold markers or on bony anatomy. These registrations assumed translational shifts only. Subsequently the dose distribution was re-calculated on the repeat scans to account for differences in patient anatomy, including organ/target motion and deformations as well as tissue heterogeneities. Dose accumulation based on deformable registration was not performed [21].

The evaluation of the sensitivity towards inter-fractional anatomy changes was made comparing the planned to the simulated dose to the CTVs. For each CTV, the physical parameters for the dose received by 99% of the target volume ( $D_{99}$ ) and the generalized equivalent uniform dose (gEUD) calculated with the dose-volume parameter  $a$  set to  $-20$  [17,22–24] were analyzed.

## **Results**

Planning constraints were fulfilled for both targets and organs at risk for most plan combinations. For planning of these challenging patients, the hardest constraint to meet was the rectum volume receiving 74 GyE with the SEQ planning technique. The proximity

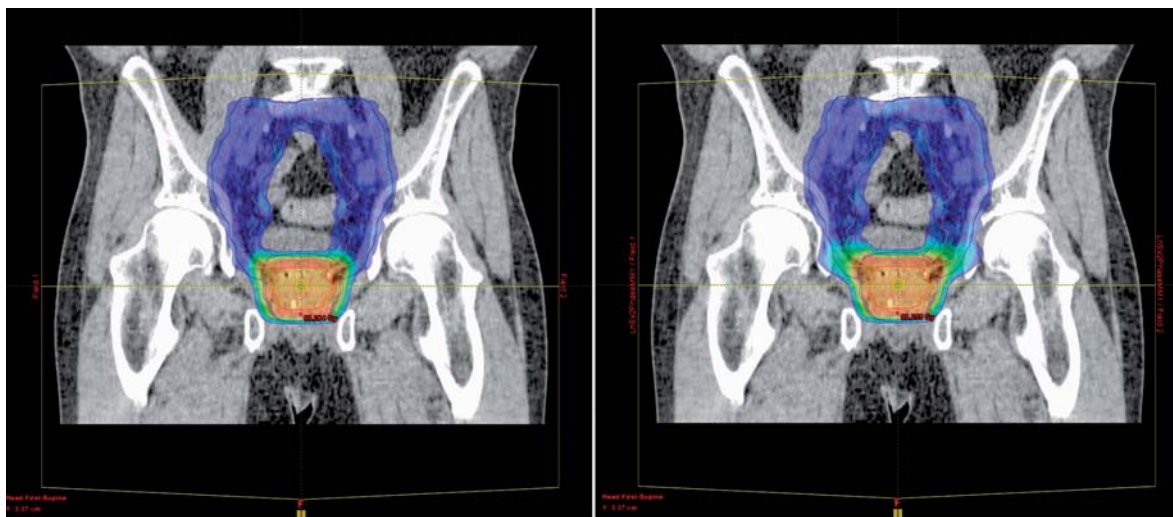


Figure 2. Sagittal view of IMPT dose distributions for SIB (left) and SEQ (right) delivery techniques for patient 3. The segmented contours of CTV-p (red), CTV-In (pink) and the PTVs (blue) are displayed and overlaid with a dose colorwash. The colorwash ranges from 95% of the prescribed dose to PTV-In/sv (blue) to 95% of the prescribed dose to PTV-p (orange).

of the prostate resulted in CTV-sv in general having a larger dose variation resulting in high doses (above the prescription for CTV-p) after plan summation of the boost and the whole pelvic fields.

Overall similar patterns in planned as compared to simulated physical dose were seen for both SEQ and SIB delivery. Comparing these two techniques revealed that although the plans were not significantly different the degradation was most pronounced for SIB delivery. However, the deviations were small, with average dose differences in  $D_{99}$  between SEQ and SIB of 0.1 GyE for CTV-p, 0.6 GyE for CTV-sv and 0.2 GyE for CTV-ln. In the following we therefore present numerical results for SIB delivery only.

For CTV-p, a margin of 4 mm was sufficient to maintain the planned  $D_{99}$  and gEUD for all patients when positioning was based on fiducial markers (Table I, Figure 3). However, with positioning based on bony anatomy, one of the four patients (patient no. 2) would have experienced an average degradation in the  $D_{99}$  for the CTV-p of  $-8.1$  GyE with a 4 mm margin. A 7 mm margin was sufficient to maintain the planned  $D_{99}$  and gEUD in all patients also with bony anatomy-based positioning.

For the seminal vesicles, large variation in the simulated  $D_{99}$  and gEUD endpoints was seen independent of positioning strategy (Table I). There was a large variation between patients (Figure 3) where patient no. 2 again had a large difference in simulated versus planned gEUD with an average of  $-31.7$  GyE and  $-38.0$  GyE for the largest margin and positioning based on fiducials and bony anatomy, respectively. For the remaining three patients a 7 mm margin was sufficient to ensure both  $D_{99}$  and gEUD dose degradations being 1.6 GyE or less.

For the lymph node target, dose degradations were seen for both positioning strategies, but with bony anatomy-based set-up being slightly better (Table I). Interestingly, the average difference between planned and simulated  $D_{99}$  was  $-2.4$  GyE (Table I), even when using a 10 mm margin and positioning based on bony anatomy. This was due to large differences between planned and simulated  $D_{99}$  in one patient. For the three remaining patients, the planned gEUD was maintained for

both positioning strategies when using a 10 mm margin (Figure 3).

## Discussion

In this study we have investigated the influence of inter-fractional motion on the dose coverage with protons for the three targets irradiated in patients with locally advanced prostate cancer. Across all targets the dose to the prostate was most robust, in particular, when positioning was based on fiducials. For the seminal vesicle target, a substantial variation in delivered dose was found independent of the positioning strategy. This was also the target where inter-patient variations had the greatest impact on both  $D_{99}$  and gEUD. For the lymph node target, positioning on bony anatomy was slightly better than positioning based on fiducials, however, the clinical relevance of this difference is uncertain.

One of the four patients had a particularly large reduction in simulated versus planned dose. This was most likely caused by an enlarged (gas-filled) rectum in the planning CT (Figure 1 left). The rectum volume of this patient was on average 48% lower in the repeat CT scans than in the planning CT. Difficulties in adequate coverage of the seminal vesicles in proton RT have also been reported previously by Zhang et al. [25]. An earlier IMPT robustness study that was limited to treatment of the prostate only with bony anatomy-based set-up also found variation in rectal volume to be a significant factor for degradation of the delivered dose to the prostate [26]. These authors further suggested increasing the robustness to organ motion by overwriting air cavities using the HU equivalent to water. Use of a rectal balloon in proton RT would have the same effect but could also reduce the amount of organ motion to limit subsequent dose degradations [26,27]. With positioning based on fiducials, degradation in dose to CTV-p was, however, not observed in our study even for the tightest margin of 4 mm.

Interestingly, our results showed that the systematic change in rectum volume influenced not only the dosimetric endpoints for the CTV-sv but also the CTV-ln. Consequently, a 10 mm margin was not

Table I. Patient average difference (and range) in delivered versus planned  $D_{99}$ .

		Fiducials [GyE]			Bony anatomy [GyE]		
		4 mm	7 mm	10 mm	4 mm	7 mm	10 mm
SIB	CTV-p	-0.6	-0.3	-0.5	-2.5	-1.1	-1.0
		(-0.3 to -1.0)	(0.0 to -1.0)	(0.2 to -1.5)	(-0.4 to -8.1)	(-0.2 to -3.9)	(0.0 to -3.6)
	CTV-sv	-9.1	-8.0	-7.0	-11.9	-9.4	-8.1
		(1.6 to -35.1)	(1.8 to -31.8)	(3.9 to -31.1)	(1.0 to -39.2)	(1.7 to -36.4)	(4.2 to -35.9)
	CTV-ln	-3.1	-2.9	-3.2	-2.0	-2.3	-2.5
		(-0.4 to -8.1)	(-0.2 to -7.6)	(-0.1 to -9.1)	(-0.2 to -5.9)	(-0.1 to -7.0)	(-0.2 to -7.8)



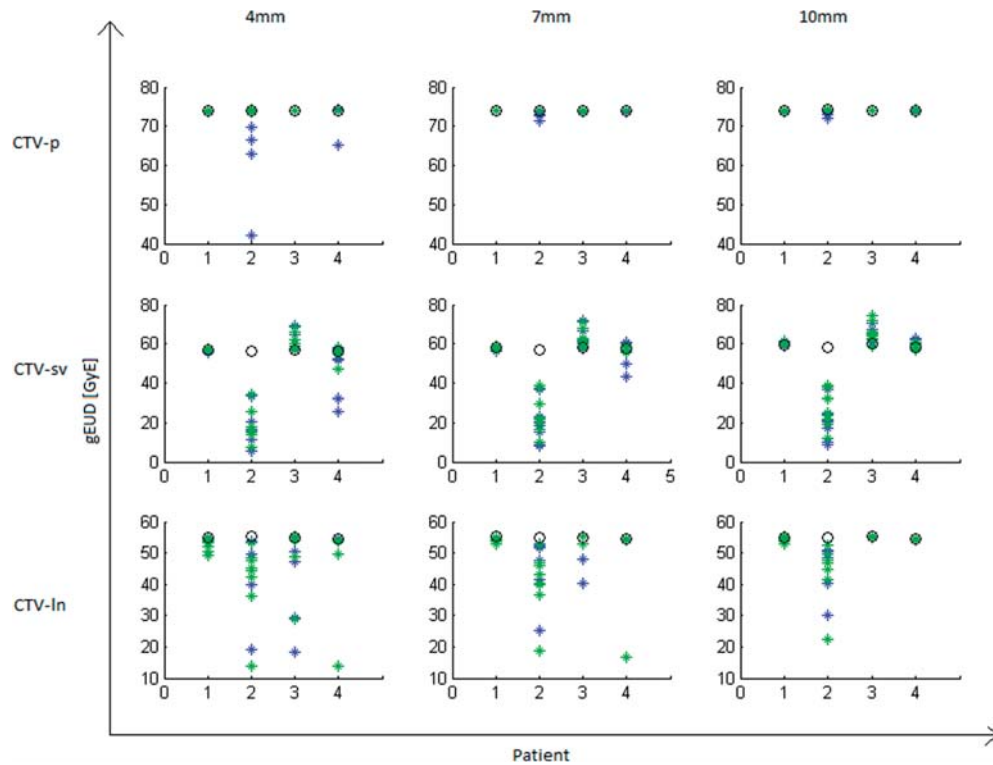


Figure 3. The planned and simulated gEUDs for each patient for the SIB plans. Planned doses are denoted by black circles, bony anatomy-based set-up are in blue and fiducial-based set-up are in green markers.

sufficient to maintain the planned CTV-In  $D_{99}$ /gEUD for this patient, even with positioning based on bony anatomy. The results of this particular patient further illustrates that a larger margin expansion around the target in proton therapy does not necessarily lead to a more robust dose distribution. Indeed, the PTV concept may not translate from RT with photons to protons since the assumption of the spatial dose distribution being invariant to geometrical changes in the beam path for photons is violated with protons [28–30]. However, in this study we used the concept of uniform expansions as a simple tool to evaluate to what extent the three targets are affected by organ motion.

In the generation of our IMPT plans we used two lateral opposing fields with planning objectives and constraints in the optimization similar to those used for photon RT. Beam configurations with two lateral opposing fields were chosen since this is currently the standard approach in proton therapy for prostate cancer [3,31,32]. Other beam configurations and spot distributions not explored in this study for generation of proton plans might lead to treatment plans that are more or less robust to inter-fraction motion [33].

In our previous IMRT target robustness study including the cases selected for the present study, we also found the largest dose degradations in the seminal vesicles – on average a relative reduction in  $D_{99}$

of 3% for bony anatomy and 5% for fiducial set-up. In the present IMPT study corresponding average degradations of 15% and 13% were obtained for simulations of SIB plans even with the largest margins. The dose degradations for the pelvic lymph node targets with proton delivery (4–5% with bony anatomy and 5–6% with fiducial set-up, across all margins) were indeed more comparable to those obtained for the seminal vesicles using IMRT. For delivery with both photons and protons it was the patient with a systematic reduction in rectum volume that were most challenging and, e.g.  $D_{99}$  for seminal vesicles in the remaining cases had degradations within 1% for photons versus 3% for protons, using comparable margins.

A particular strength of this study is the use of a solid repeat image material (8–9 CT scans for each patient) capturing organ and target motion patterns that are likely to have also been present during treatment delivery. However, intra-fraction motion, set-up errors as well as rotational effects might influence the estimated delivered doses. In addition, delineation uncertainties might also have an effect on the results. We aimed to minimize this effect by having all delineations performed by one radiation oncologist. Besides, the study is limited by a modest number of patients, making it difficult to draw definitive general conclusions on the overall influence of changes in anatomy for this treatment scenario. Nevertheless, by

selecting patients presenting large organ motion we still were successful in providing an estimate of the range of degradation that could be present for this group of patients.

In conclusion, this study found the largest dose degradation for the seminal vesicle target independent of set-up strategy. Although most of the patients presented small differences in delivered as compared to planned dose for both the lymph node and seminal vesicle targets, the dose degradation was substantial for a patient with a systematic reduction in rectum volume. This was independent of margin expansion and patient positioning. The prostate target was found robust to such changes when fiducial-based positioning was used.

### Acknowledgments

Varian Medical Systems is thanked for providing the proton dose calculation software.

**Declaration of interest:** The authors report no conflicts of interest. The authors alone are responsible for the content and writing of the paper.

This work has been supported by research grants from CIRRO – The Lundbeck Foundation Center for Interventional Research in Radiation Oncology, the Danish Cancer Society, FSS (The Danish Council for Independent Research) as well as the Danish Council for Strategic Research.

### References

- [1] Dearnaley DP, Sydes MR, Graham JD, Aird EG, Bottomley D, Cowan RA, et al. Escalated-dose versus standard-dose conformal radiotherapy in prostate cancer: First results from the MRC RT01 randomised controlled trial. *Lancet Oncol* 2007;8:475–87.
- [2] Peeters ST, Heemsbergen WD, van Putten WL, Slot A, Tabak H, Mens JW, et al. Acute and late complications after radiotherapy for prostate cancer: Results of a multicenter randomized trial comparing 68 Gy to 78 Gy. *Int J Radiat Oncol Biol Phys* 2005;61:1019–34.
- [3] Coen JJ, Bae K, Zietman AL, Patel B, Shipley WU, Slater JD, et al. Acute and late toxicity after dose escalation to 82 GyE using conformal proton radiation for localized prostate cancer: Initial report of American College of Radiology Phase II study 03-12. *Int J Radiat Oncol Biol Phys* 2011;81:1005–9.
- [4] Coen JJ, Paly JJ, Niemierko A, Weyman E, Rodrigues A, Shipley WU, et al. Long-term quality of life outcome after proton beam monotherapy for localized prostate cancer. *Int J Radiat Oncol Biol Phys* 2012;82:201–9.
- [5] Olsen DR, Bruland OS, Frykholm G, Norderhaug IN. Proton therapy – a systematic review of clinical effectiveness. *Radiother Oncol* 2007;83:123–32.
- [6] Nyström H, Blomqvist E, Hoyer M, Montelius A, Muren LP, Nilsson P, et al. Particle therapy – a next logical step in the improvement of radiotherapy. *Acta Oncol* 2011;50:741–4.
- [7] Vargas C, Wagner M, Mahajan C, Indelicato D, Fryer A, Falchook A, et al. Proton therapy coverage for prostate cancer treatment. *Int J Radiat Oncol Biol Phys* 2008;70:1492–501.
- [8] Zietman AL, Bae K, Slater JD, Shipley WU, Efstathiou JA, Coen JJ, et al. Randomized trial comparing conventional-dose with high-dose conformal radiation therapy in early-stage adenocarcinoma of the prostate: Long-term results from Proton Radiation Oncology Group/American College Of Radiology 95-09. *J Clin Oncol* 2010;28:1106–11.
- [9] Wang D, Lawton C. Pelvic lymph node irradiation for prostate cancer: Who, why, and when. *Semin Radiat Oncol* 2008;18:35–40.
- [10] Widesott L, Pierelli A, Fiorino C, Lomax AJ, Amichetti M, Cozzarini C, et al. Helical tomotherapy versus intensity-modulated proton therapy for whole pelvis irradiation in high-risk prostate cancer patients: Dosimetric, normal tissue complication probability, and generalized equivalent uniform dose analysis. *Int J Radiat Oncol Biol Phys* 2011;80:1589–600.
- [11] Lassen-Ramshad Y, Vestergaard A, Muren LP, Hoyer M, Petersen JB. Plan robustness in proton beam therapy of a childhood brain tumour. *Acta Oncol* 2011;50:791–6.
- [12] Johansson B, Ridderheim M, Glimelius B. The potential of proton beam radiation therapy in prostate cancer, other urological cancers and gynaecological cancers. *Acta Oncol* 2005;44:890–5.
- [13] Allen AM, Pawlicki T, Dong L, Fourkal E, Buuynouski M, Cengel K, et al. An evidence based review of proton beam therapy: The report of ASTRO's emerging technology committee. *Radiother Oncol* 2012;103:8–11.
- [14] Chera BS, Vargas C, Morris CG, Louis D, Flampouri S, Yeung D, et al. Dosimetric study of pelvic proton radiotherapy for high-risk prostate cancer. *Int J Radiat Oncol Biol Phys* 2009;75:994–1002.
- [15] Schippers JM, Lomax AJ. Emerging technologies in proton therapy. *Acta Oncol* 2011;50:838–50.
- [16] Liang J, Wu Q, Yan D. The role of seminal vesicle motion in target margin assessment for online image-guided radiotherapy for prostate cancer. *Int J Radiat Oncol Biol Phys* 2009;73:935–43.
- [17] Thörnqvist S, Bentzen L, Petersen JB, Hysing LB, Muren LP. Plan robustness of simultaneous integrated boost radiotherapy of prostate and lymph nodes for different image-guidance and delivery techniques. *Acta Oncol* 2011;50:926–34.
- [18] Thörnqvist S, Petersen JB, Hoyer M, Bentzen L, Muren LP. Propagation of target and organ at risk contours in radiotherapy of prostate cancer using deformable image registration. *Acta Oncol* 2010;49:1023–32.
- [19] Lomax A, Pedroni E, Schaffner B, Scheib S, Schneider U, Tourovsky A. 3D treatment planning for conformal proton therapy by spotscanning. In: Faulkner K, Carey B, Crellin A, Harrison RM, editors. *Quantitative imaging in oncology*. London: BIR Publishing; 1996. p. 67–71.
- [20] International Commission on Radiation Units and Measurements. Prescribing, recording and reporting proton-beam therapy (ICRU Report 78). *J ICRU* 2007;7.
- [21] Andersen ES, Muren LP, Sørensen TS, Noe KO, Thor M, Petersen JB, et al. Bladder dose accumulation based on a biomechanical deformable image registration algorithm in volumetric modulated arc therapy for prostate cancer. *Phys Med Biol* 2012;57:7089–100.
- [22] Niemierko A. Reporting and analyzing dose distributions: A concept of equivalent uniform dose. *Med Phys* 1997;24:103–10.
- [23] Niemierko A. A generalized concept of equivalent uniform dose. *Med Phys* 1999;26:1000 (Abstract).

- [24] Søvik Å, Ovrum J, Olsen DR, Malinen E. On the parameter describing the generalised equivalent uniform dose (gEUD) for tumours. *Phys Med* 2002;23:100–6.
- [25] Zhang X, Dong L, Lee AK, Cox JD, Kuban DA, Zhu RX, et al. Effect of anatomic motion on proton therapy dose distributions in prostate cancer treatment. *Int J Radiat Oncol Biol Phys* 2007;67:620–9.
- [26] Soukup M, Söhn M, Yan D, Liang J, Alber M. Study of robustness of IMPT and IMRT for prostate cancer against organ movement. *Int J Radiat Oncol Biol Phys* 2009;75:941–9.
- [27] Smeenk RJ, Teh BS, Butler EB, van Lin EN, Kaanders JH. Is there a role for endorectal balloons in prostate radiotherapy? A systematic review. *Radiother Oncol* 2010;95:277–82.
- [28] Lomax AJ. Intensity modulated proton therapy and its sensitivity to treatment uncertainties 2: The potential effects of inter-fraction and inter-field motions. *Phys Med Biol* 2008;53:1043–56.
- [29] Park PC, Zhu XR, Lee AK, Sahoo N, Melancon AD, Zhang L, et al. A beam-specific planning target volume (PTV) design for proton therapy to account for setup and range uncertainties. *Int J Radiat Oncol Biol Phys* 2012;82:329–36.
- [30] De Ruyscher D, Mark Lodge M, Jones B, Brada M, Munro A, Jefferson T, et al. Charged particles in radiotherapy: A 5-year update of a systematic review. *Radiother Oncol* 2012;103:5–7.
- [31] Nihei K, Ogino T, Onozawa M, Murayama S, Fuji H, Murakami M, et al. Multi-institutional phase II study of proton beam therapy for organ-confined prostate cancer focusing on the incidence of late rectal toxicities. *Int J Radiat Oncol Biol Phys* 2011;81:390–6.
- [32] Trofimov A, Nguyen PL, Efstathiou JA, Wang Y, Lu HM, Engelsman M, et al. Interfractional variations in the setup of pelvic bony anatomy and soft tissue, and their implications on the delivery of proton therapy for localized prostate cancer. *Int J Radiat Oncol Biol Phys* 2011;80:928–37.
- [33] Stuschke M, Kaiser A, Pöttgen C, Lübcke W, Farr J. Potentials of robust intensity modulated scanning proton plans for locally advanced lung cancer in comparison to intensity modulated photon plans. *Radiother Oncol* 2012;104:45–51.